

RESEARCH

Open Access



Polyp and tumor microenvironment reprogramming in colorectal cancer: insights from mucosal bacteriome and metabolite crosstalk

Hadi Feizi^{1,2}, Hossein Samadi Kafil^{1*}, Andrey Plotnikov³, Vladimir Kataev³, Alexander Balkin³, Ekaterina Filonchikova³, Mohammad Ahangarzadeh Rezaee⁴, Reza Ghotaslou⁴, Mohammad Sadrkabir⁵, Hiva Kadkhoda^{1,8}, Fadhil S. Kamounah⁶ and Sergei Nikitin⁷

Abstract

Background Highly frequent colorectal cancer (CRC) is predicted to have 3.2 million novel cases by 2040. Tumor microenvironment (TME) bacteriome and metabolites are proposed to be involved in CRC development. In this regard, we aimed to investigate the bacteriome and metabolites of healthy, adenomatous polyp, and CRC tissues.

Methods Sixty samples including healthy (H), adenomatous polyps (AP), adenomatous polyps-adjacent (APA), cancer tumor (CT), and cancer tumor-adjacent (CA) tissues were collected and analyzed by 16 S rRNA sequencing and ¹H NMR spectroscopy.

Results Our results revealed that the bacteriome and metabolites of the H, AP, and CT groups were significantly different. We observed that the Lachnospiraceae family depleted concomitant with acetoacetate and beta-hydroxybutyric acid (BHB) accumulations in the AP tissues. In addition, some bacterial species including *Gemella morbillorum*, and *Morganella morganii* were enriched in the AP compared to the H group. Furthermore, fumarate was accumulated concomitant to *Aeromonas enteropelogenes*, *Aeromonas veronii*, and *Fusobacterium nucleatum* subsp. *animalis* increased abundance in the CT compared to the H group.

Conclusion These results proposed that beneficial bacteria including the Lachnospiraceae family depletion cross-talk with acetoacetate and BHB accumulations followed by an increased abundance of driver bacteria including *G. morbillorum*, and *M. morganii* may reprogram polyp microenvironment leading to tumor initiation. Consequently, passenger bacteria accumulation like *A. enteropelogenes*, *A. veronii*, and *F. nucleatum* subsp. *animalis* cross-talking fumarate in the TME may aggravate cancer development. So, knowledge of TME bacteriome and metabolites might help in cancer prevention, early diagnosis, and a good prognosis.

Keywords Colorectal cancer, Gut microbiome, Gut metabolome, Tumor microenvironment, *Fusobacterium nucleatum*

*Correspondence:
Hossein Samadi Kafil
kafilhs@tbzmed.ac.ir

Full list of author information is available at the end of the article



© The Author(s) 2025. **Open Access** This article is licensed under a Creative Commons Attribution-NonCommercial-NoDerivatives 4.0 International License, which permits any non-commercial use, sharing, distribution and reproduction in any medium or format, as long as you give appropriate credit to the original author(s) and the source, provide a link to the Creative Commons licence, and indicate if you modified the licensed material. You do not have permission under this licence to share adapted material derived from this article or parts of it. The images or other third party material in this article are included in the article's Creative Commons licence, unless indicated otherwise in a credit line to the material. If material is not included in the article's Creative Commons licence and your intended use is not permitted by statutory regulation or exceeds the permitted use, you will need to obtain permission directly from the copyright holder. To view a copy of this licence, visit <http://creativecommons.org/licenses/by-nc-nd/4.0/>.

Introduction

Colorectal cancer (CRC) was the third most common malignancy (9.6% of all cancer incidence), and the second deadliest cancer (9.3% of all cancer-related mortality) worldwide by 2022. Transitioned countries have 3–4 times higher incidence rates than transitioning countries with a progressively increasing rate in countries undergoing major transition including South America, South-Eastern and South-Central Asia, and Eastern Europe countries [1]. There is also an incidence rising shift in the younger (individuals less than 50 years) people known as early-onset colorectal cancer (EOCRC) [2]. Different patterns of incidence in distinct geographical locations propose the critical role of environmental risk factors in CRC incidence. Specifically, it is suggested that CRC is largely affected by several modifiable risk factors like colorectal bacteriome and metabolome [3].

The role of colorectal microbiota and especially gut bacteriome is becoming increasingly evident in CRC pathogenesis as a modifiable risk factor [4]. Several studies demonstrated distinct bacterial profiles in CRC patient's stools at various taxonomic levels in comparison to healthy individuals [5]. Other researchers also observed tumor-specific bacterial profiles in the different stages of CRC [6]. On the other hand, tumor microenvironment (TME) metabolome alterations are also considered a critical hallmark of CRC [7]. There are numerous microbial-derived metabolites in human cells, tissues, organs, or biological fluids that have correlations with malignancies [8]. It was shown that fecal metabolites might have significant roles in CRC initiation [9]. While most of the previous studies tried to evaluate the bacteriome and metabolome of CRC patients, some of them used fecal samples which were concluded not to be indicators of the TMEs [10]. Moreover, adenomatous polyps (precancerous stage) as the origination of about 95% of the CRC [11] were excluded in several studies. On the other hand, it was found that peri-operative interventions in patients undergoing surgery including antibiotic or other medication usage, nutrition type, surgical stress, and injury might affect the TMEs bacteriome and metabolome [12]. So, mucosal tissue sampling during endoscopy is preferred to post-operative tissue collection and also fecal samples [13]. Furthermore, although bacteriome-metabolome interactions and cross-talk evaluation are crucial steps toward understanding CRC pathogenesis mechanisms [14], few researchers conduct bacteriome-metabolome studies regarding CRC. Considering the preceding information, the goal of our study is to evaluate the age and sex-matched healthy gut, adenomatous polyps, and colorectal cancer tumor mucosal bacteriome and metabolome composition and their correlations.

Materials and methods

Study populations and sample collection

From January 2022 to March 2023, 14 CRC patients, 6 adenomatous polyps patients, and 20 healthy individuals were recruited from Tabriz hospitals (Table S1). The protocols described in this document were approved by the Tabriz Regional Ethics Committee (Tabriz University of Medical Sciences, Tabriz, Iran), No. I.R.TBZMED.REC.1400.155. All the procedures were done according to the Helsinki Declaration, and study participants obtained informed consent before the endoscopy, and samples were collected during the endoscopy process. None of the participants who underwent endoscopic procedures used antiplatelet or anticoagulants. This experiment randomly matched participants according to age and gender. Participants in this study did not receive antibiotics, neoadjuvant chemotherapy, or radiation therapy three months before the endoscopic process.

Colorectal cancer tumors (CT), adenomatous polyps (AP), and adjacent normal-appearing tissues (5–10 cm away from the edges of CT and AP) including cancer tumor adjacent (CA) and adenomatous polyp adjacent (APA) were collected from CRC and AP patients undergoing primary endoscopy without medical alterations. The bowel preparations were carried out by advising the participants to drink 4 L of a polyethylene glycol-electrolyte solution (Pidrolax 4000, SEPIDAJ, Tehran, Iran). All colonoscopies were performed using standard electronic video colonoscopes (BL-7000/VP-7000; FUJIFILM Corporation, Tokyo, Japan). All tissues were taken with oval fenestrated spike biopsy forceps (ENDO-FLEX GmbH, Germany) with a 2.3 mm outer diameter. Each biopsy specimen's weight was approximately 10 mg. Normal tissues were taken from healthy individuals (H) who had been referred to endoscopy electively with the diagnosis of a specialist doctor according to indications such as abdominal pain. These individuals were diagnosed as completely healthy by performing blood tests and endoscopy by a specialist doctor and filling out a complete questionnaire about any history of chronic diseases, antibiotic usage in the last 3 months, familial colorectal cancer, and demographic data.

A blinded specialist obtained 60 tissue samples (14 CT, 14 CA, 6 AP, 6 APA, and 20 H) from CRC, adenomatous polyp, and healthy participants. These tissues were washed with sterile NaCl 9% and immediately transferred to -80°C for further metabolic analysis. For 16s rRNA sequencing, tissue samples were immersed in the RNA lysis solution (Yekta Tajhiz Azma, Iran) before storing them at -80°C . The clinical diagnosis, tumor stage, and histological differentiation were determined by routine histopathology examination of the samples by a blinded pathologist.

Sample preparation for ¹H-NMR spectroscopic analysis

Frozen tissue specimens were weighed and suspended in methanol (Merck, Germany [4 mL per gram of tissue]) and double-distilled water (0.85 mL/gram of tissue). After the vortex, chloroform (Merck, Germany [2 mL/gram of tissue]) was added, followed by the addition of 50% chloroform (2 mL/gram of tissue). The suspension was incubated on ice for 30 min and centrifugated at 1,000 × g for 30 min at 4 °C. Each specimen's aqueous phase (upper phase) was collected and evaporated to dryness under a stream of nitrogen. The residue was freeze-dried with a freeze dryer (Epsilon 1–4 LSC plus, Germany). The residue was reconstituted with 580 μL of D₂O containing 30 μM phosphate buffer solution (PBS, pH=7.4) and 0.01 mg/ml sodium (3-trimethylsilyl)-2, 2, 3, tetradeuteriopropionate (TSP) as a chemical shift reference (δ0.0). After centrifuging at 12,000 × g for 5 min, the 550 μL supernatant was transferred into a 5-mm NMR tube for NMR spectroscopy [15].

¹H-NMR spectroscopic analysis

Sixty tissue samples, including healthy (H), cancer tumor (CT), cancer tumor-adjacent (CA), adenomatous polyps (AP), and adenomatous polyps adjacent (APA) were analyzed by ¹H NMR spectroscopy at 25°C on a Bruker AVANCE III™ 500 MHz CRYO probe instrument (Bruker Biospin GmbH, Rheinstetten, Germany). The starting reagents and solvents were purchased from Sigma-Aldrich and used as received. The solvents used for the experimental NMR analysis (HPLC grade) were purchased from Sigma-Aldrich. All other materials were commercial products of analytical grade and used as supplied. PBS buffer pH 7.4 was prepared by dissolving KH₂PO₄ (5.1 mg), KCl (4.4 mg), Na₂HPO₄·H₂O (37.6 mg), and NaCl (161.3 mg) in 20 mL D₂O. The pH was adjusted to 7.4 by adding NaOH (1 M in D₂O). Experimental parameters were: TD=65536, NS=256, DS=2, D1=1 sec, SW=20.0254 ppm, O1P=6.175 ppm, 1TD=65536, TE=298 K. Chemical shifts are reported in ppm relative to an external standard TSP (δ0.0 ppm in D₂O). All the ¹H-NMR spectra were corrected for phase and baseline distortions using MestReNova-14.3.3-33362 software. All metabolites' overviews were provided by the standard one-dimension spectra. The major metabolites in the spectra ranging from 0.5 to 9.5 ppm were identified according to literature data and the Human Metabolome Database (<http://www.hmdb.ca/>). The region 4.6–4.9 ppm was removed to exclude the effect of imperfect water signal.

Nontargeted metabolite profiling and data processing methods

Identified metabolites in different study groups were analyzed using two modules (statistical analysis [single

factor], and enrichment analysis modules) of a web-based platform for the comprehensive analysis of quantitative metabolomic data, MetaboAnalyst 6.0 (www.metaboanalyst.ca [accessed on February 2024]). The Orthogonal partial least squares-discriminant analysis (OPLS-DA) score plots, S-plots, VIP (variable importance in projection) plots, and significant analysis of metabolites (SAM) were used to improve the study group's separation. The robustness and validity of the OPLS-DA model were assessed using the 2000-permutation test. Taxon Set Enrichment Analysis (TSEA) was also set to identify significantly related diseases to CT tissues metabolites group using metabolites sets reported in MetaboAnalyst 6.0. The disease signatures were shown according to their enrichment ratio and *p*-values.

Sample preparation and total DNA extraction for 16 S rRNA sequencing

Genomic DNA extraction from the specimens was done using the SkyAmp micro DNA kit (Skygen, Russia) according to the modified protocol. The initial steps of the protocol were modified in the following way. Lysis Matrix Y (MP Biomedicals, USA), and tissue fragments were placed into 1.5 mL Safe-Lock microcentrifuge tubes (Eppendorf, Hamburg, Germany), followed by immediate addition of 180 μL of GA Buffer and homogenization for 5 min at 50 Hz in Qiagen TissueLyser LT (Qiagen, Hilden, Germany). Other steps were performed strictly according to the DNA extraction protocol. Particularly, 20 μL of Proteinase K was added and vortexed for 10 s. After that, specimens were incubated at 56 °C for 30 min in a CH-100 Heating/Cooling Dry Block (BioSan, Latvia). Next, 200 μL of GB Buffer and 1 μL of the carrier RNA stock solution (1 μg/μL) were added, and tubes were incubated at 70 °C for 10 min. Subsequently, 200 μL of ice-cold ethanol was added and tubes were incubated at room temperature for 5 min. The lysates were transferred to the spin columns (in 2 mL collection tubes) and centrifuged for 30 s at 13,400 × g. After that the supernatants were discarded, 500 μL of GD Buffer was added in every spin column and centrifuged for 30 s at 13,400 × g. The last step was repeated twice with 600 μL of PV Buffer. Then, the spin columns were centrifuged for 2 min and incubated at room temperature for 5 min. Finally, the spin columns were placed into new 1.5 mL tubes. Twenty-five μL of TB Buffer was added in the center of a membrane in every column, and incubated for 5 min at 37 °C, followed by centrifuging for 2 min to collect purified DNA. The quality of the extracted DNA was evaluated using 1% agarose gel electrophoresis and a Nanodrop 8000 spectrophotometer (Thermo Fisher Scientific, Waltham, MA, USA) at OD260/OD280. Qubit 4.0 Fluorometer and dsDNA High Sensitivity Assay Kit (Thermo Fisher

Scientific, Waltham, MA, USA) were used to measure the DNA concentration.

Library construction and sequencing

Preparation of the DNA libraries was performed according to the Illumina protocol (Part #15044223, Rev. B.) with primers targeting the V3–V4 regions of the SSU ribosomal RNA (rRNA) gene, S-D-Bact-0341-b-S-17 (5'-CCTACGGGNGGCWGCAG-3') as the forward primer and S-D-Bact-0785-a-A-21 (5'-GACTACH-VGGGTATCTAATCC-3') as the reverse primer [<https://doi.org/10.1093/nar/gks808>]. Twenty-five μ L of the reaction mixture contained both primers (0.4 μ L each), 1.25 μ L dNTPs, 0.13 μ L Q5 High-Fidelity DNA Polymerase (New England Biolabs, USA), 3.75 μ L Q5 buffer, and 3 μ L sample DNA. PCR was performed in triplicates for every sample with the following program: 95 °C for 3 min, 25 cycles 95 °C for 30 s, 56 °C for 30 s, 72 °C for 30 s, and final extension 72 °C for 5 min. The amplicons from triplicates were mixed and cleaned up using Agencourt AMPure XP beads (Beckman Coulter, Brea, CA, USA). The adapters and indices were attached to the amplicons according to the Illumina protocol (Part #15044223, Rev. B). The DNA libraries were validated using real-time PCR, normalized, and pooled. Paired-end 2 \times 250 bp sequencing was performed on the MiSeq platform (Illumina, San Diego, CA, USA) with the Reagent Kit v.2 (Illumina, San Diego, CA, USA).

Bioinformatics and statistical treatment of DNA metabarcoding data for bacteriomes

Raw reads were trimmed against primers using Cutadapt v. 4.1 [16]. Then, reads were processed (sequence quality control, trimming, and chimera removal), and exact sequence variants (ESVs, named as zOTUs - operational taxonomic units by the authors of the tool) were generated using the denoising algorithm UNOISE implemented in USEARCH v.11 [17]. The naive Bayesian classifier against the GTDB database (release 207) [18] was used for the taxonomy assignment of ESVs. ESVs assigned to Eukaryotes or unclassified at the kingdom level were removed. Alpha diversity was applied to analyze taxa diversity within a sample through the number of observed ESVs, Shannon diversity index, and Chao1 richness, as diversity measures and T-test/ANOVA as a statistical method. To analyze how closely related the samples were to each other, beta diversity analyses were determined based on the Bray-Curtis dissimilarities, Jensen-Shannon Divergence, Unweighted and Weighted UniFrac phylogenetic as distance metrics, and PERMANOVA (Permutational multivariate analysis of variance) as the statistical method. All distances were visualized using the ordination-based method of non-metric multidimensional scaling (NMDS) into

two-dimensional plots. To detect the most frequent signatures of a list of bacterial genera and species with host-intrinsic taxon sets such as diseases, the TSEA (Taxon Set Enrichment Analysis) module was used to enable hypothesis generation and data interpretation by performing hypergeometric tests of interest data. Differential expression analysis for sequence count data v. 2 (DESeq2) with adjusted cutoff p -value < 0.05 was used to identify differences in taxa (including genus and species) abundances of different studied groups [19]. A correlation heatmap of colorectal tissue's bacteriome-metabolome was also created. Data was scaled via autoscaling as normalization and distance correlation test was used as similarity method. Features with a p -value less than 0.01 and correlations more than 0.35 were considered significant. The Microbiome Analyst 2.0 platform [16] was used to perform the diversity and compositional analysis, as well as comparative analysis based on the ESVs table from the 16 S rRNA sequencing data, and bacteriome-metabolome correlation analysis of our study. The ESVs abundance table was filtered with counts smaller than 4 and 10% prevalence as low read counts due to probable sequencing errors or low-level contaminations. 10% of the feature's lowest percentage was also excluded using the inter-quantile range (IQR) as a low variance filter.

Results

1H-NMR spectroscopic analysis

The aqueous phase extracts of different study groups (H, CA, CT, AP, and APA) metabolites were shown in Fig. 1. These metabolites included acetate, acetoacetate, acetone, alanine, betaine, glucose, phosphocholine/choline, phosphocreatine/creatine, dimethylglycine, formate, formic acid, fumarate, glutamine, glutaric acid, guanine, inosine, isoleucine, lactate, leucine, lysine, methylamine, myo-inositol, o-acetyl glycoprotein, phenylalanine, serine, succinate, scyllo-inositol, taurine, threonine, trimethylamine-N-oxide, tyrosine, uracil, valine, and beta-hydroxybutyric acid (BHB).

16 S rRNA sequencing

A rarefaction analysis was performed for each colorectal tissue sample sequence dataset resulting in the rarefaction curves that were smooth and reached a plateau for most of the samples except for AP7 and APA7 (Fig. 2A). The numbers of samples obtained from H, CT, CA, AP, and APA groups were 20, 14, 14, 6, and 6, respectively (a total of 60 samples). The 16 S rRNA gene fragment sequencing generated a total of 2,219,316 read counts, with an average of 37,615 reads per sample (maximum and minimum counts per sample were 49,220, and 24,481, respectively). The total ESV number obtained was 1,687, and 1,478 of these ESVs had a size of more than 2 reads. The average numbers of reads for samples

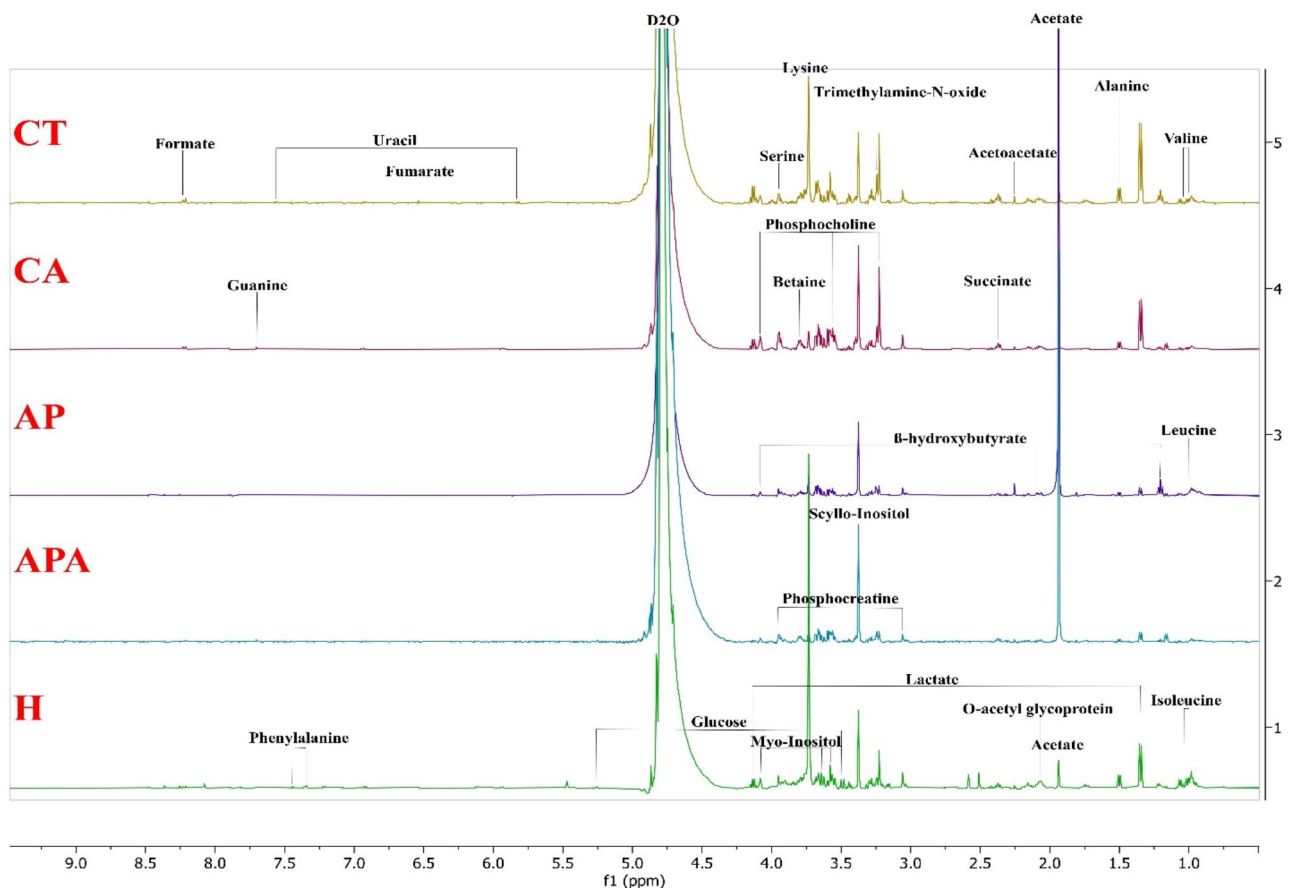


Fig. 1 Some of 500 MHz representative ^1H NMR spectra ($\delta 0.5\text{--}8.5$) of different study group's tissue sample metabolites. 1: healthy individuals (H), 2: adenomatous polyps adjacent (APA), 3: adenomatous polyps (AP), 4: cancer tumor adjacent (CA), and 5: cancer tumor (CT)

of H, CA, CT, APA, and AP were 37,560; 38,471; 37,591; 42,817; and 31,532, respectively. The average numbers of ESVs per sample for H, CA, CT, APA, and AP groups were 173, 144, 135, 284, and 239, respectively. The average of every ESV counts per sample for H, CA, CT, APA, and AP groups were 250, 296, 313, 225, and 201, respectively (Fig. 2B and Table S2).

Bacteriome analysis using bioinformatics tools

Significantly different colorectal bacteriome alpha diversity metrics were observed between the studied groups. As it was shown in Fig. 3A-C, the alpha diversity decreased throughout CT, CA, H, APA, and AP groups, respectively. This was attributed to the richness as indicated by the Chao1 index (p -value 0.01811; F -value 3.2628), and observed species (p -value 0.010908; F -value 3.6255) (Fig. 3A, and 3B, respectively), as well as to diversity assessed by the Shannon index (p -value 0.011059; F -value 3.6156) between the studied groups (Fig. 3C). The highest alpha diversity of colorectal bacteriomes was related to the CT group, whereas the lowest alpha diversity was related to the AP group. The most significant differences in alpha diversities were between CT and

AP. There were also significant differences between the H group compared to CA, CT, APA, and AP groups. Moreover, there were no significant differences in alpha diversity between CA compared to CT, and APA compared to the AP group (Table S3).

NMDS was used to evaluate the beta diversity of the colorectal bacteriomes based on Bray-Curtis (Fig. 3D), Jensen-Shannon Divergence (Fig. 3E), Unweighted UniFrac (Fig. 3F), and Weighted UniFrac (Fig. 3G) distance matrices and showed significant differences between most studied groups. Based on the Bray-Curtis index as the distance method and PERMANOVA as the statistical method, there were significant differences in beta diversities between H vs. CT (F -value: 2.65, FDR :0.01), H vs. CA (F -value: 2.55, FDR :0.01), H vs. AP (F -value: 2.24, FDR :0.01), and H vs. APA (F -value: 2.03, FDR :0.02) (Fig. 3D). Based on the Jensen-Shannon Divergence as distance method, there were also significant differences in beta diversities between H vs. CT (F -value: 3.36, FDR :0.01), H vs. CA (F -value: 2.94, FDR :0.01), H vs. APA (F -value: 2.79, FDR :0.02), and H vs. AP (F -value: 2.16, FDR :0.04) (Fig. 3E). Based on the Unweighted UniFrac as distance method, there were significant differences in

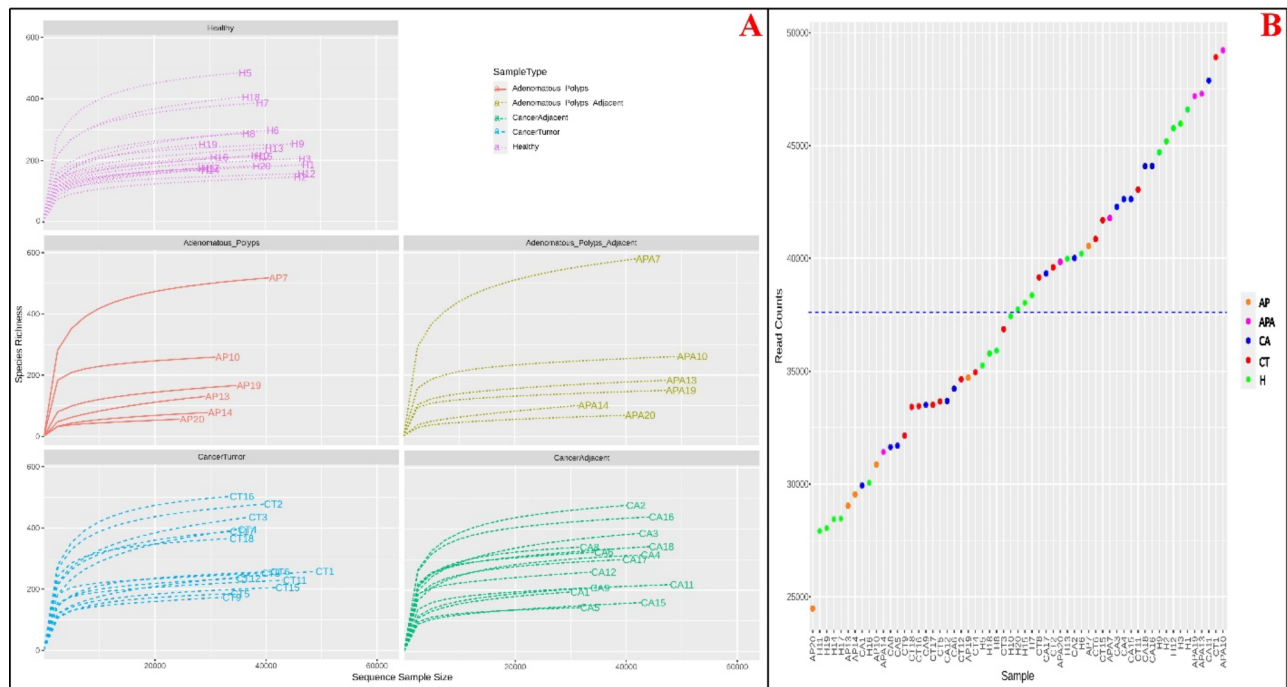


Fig. 2 Bacteriome rarefaction curves and library size for studied samples. Rarefaction curves (A) and library size view (B) of 5 different studied groups including H (healthy), CA (cancer tumor adjacent), CT (cancer tumor), AP (adenomatous polyps), and APA (adenomatous polyps adjacent) represented according to feature abundance table containing raw counts. In the rarefaction curves the vertical axis shows the number of ESVs, and the number of reads is shown on the horizontal axis

beta diversities between CT vs. AP (F-value: 2.68, FDR: 0.04), H vs. CT (F-value: 2.47, FDR: 0.04), CT vs. APA (F-value: 2.42, FDR: 0.04), CA vs. AP (F-value: 2.25, FDR: 0.04), and H vs. AP (F-value: 2.10, FDR: 0.04) (Fig. 3F). Based on the Weighted UniFrac as distance method, there were significant differences in beta diversities only between H vs. AP (F-value: 4.03, FDR: 0.05), and H vs. CT (F-value: 2.72, FDR: 0.05) (Fig. 3G) (Table S4).

The bacterial composition of colorectal tissues was classified into 12 phyla, 14 classes, 29 orders, 59 families, 193 genera, and 325 species using stacked bar plots as summarized in Fig. 4. Firmicutes-A (formerly known as Bacillota-A) was the most abundant phylum in all studied groups except the APA group (45.8%, 41%, 40.1%, 34.1%, and 32.6% in the H, CT, CA, AP, and APA groups, respectively). Bacteroidota was the second most abundant phylum (39.5%, 33.5%, 30.9%, 29.8%, and 29.3% in the APA, CA, CT, H, and AP groups, respectively). The highest proportions of the Fusobacteriota phylum were related to the AP (11.7%) and CT groups (4.1%), whereas the H and APA groups had the smallest proportions (0.52% and 0.12%, respectively). Among all groups, only bacteriomes of the CT group had representatives of Campylobacterota phylum (0.41%). Total proportions of three phyla including Firmicutes-A, Bacteroidota, and Proteobacteria were higher in non-cancerous tissue groups (H, CA, and APA) in contrast to CT and AP groups (89.7%, 89.3,

and 95.4% compared to 85.9% and 83%, respectively). The Firmicutes/Bacteroidota (F/B) ratios were 1.77, 1.53, and 1.32 for the H, CT, and AP groups, respectively. (Fig. 4A). At the class level, Clostridia, Bacteroidia, and Gammaproteobacteria were the most abundant classes (with an average of 38.7, 32.6, and 17.2, respectively). Fusobacteriia had higher proportions in AP and CT compared to CA, H, and APA (11.76%, 4.1%, opposite to 1.7%, 0.52%, and 0.12%, respectively) (Fig. 4B). Bacteroidales was the most abundant order among all studied groups except for the H group, in which the Lachnospirales was the most abundant (33.2% of Lachnospirales in comparison to 29.8% of Bacteroidales). Enterobacterales order had higher proportions in the AP and APA groups in comparison to other groups. Fusobacteriales order had higher proportions in AP and CT in contrast to CA, APA, and H groups (13.34%, 2.69%, 1.23%, 0.13%, and 0.33%, respectively). Clostridiales order had higher proportions in AP and APA in comparison to H, CT, and CA (13.15%, 10.8%, 0.9%, 0.98%, and 0.15%, respectively). Campylobacterales order was only present in the CT group (0.04%) (Fig. 4C). At the family level, Fusobacteriaceae family proportions decreased sharply throughout AP, CT, CA, H, and APA groups (13.3%, 2.7%, 1.2%, 0.3%, and 0.1%, respectively). The Clostridiaceae family was predominant in AP and APA in contrast to CT, H, and CA (11.5%, 10.05%, 0.83%, 0.81%, and 0.13%, respectively). *Enterobacteriaceae*

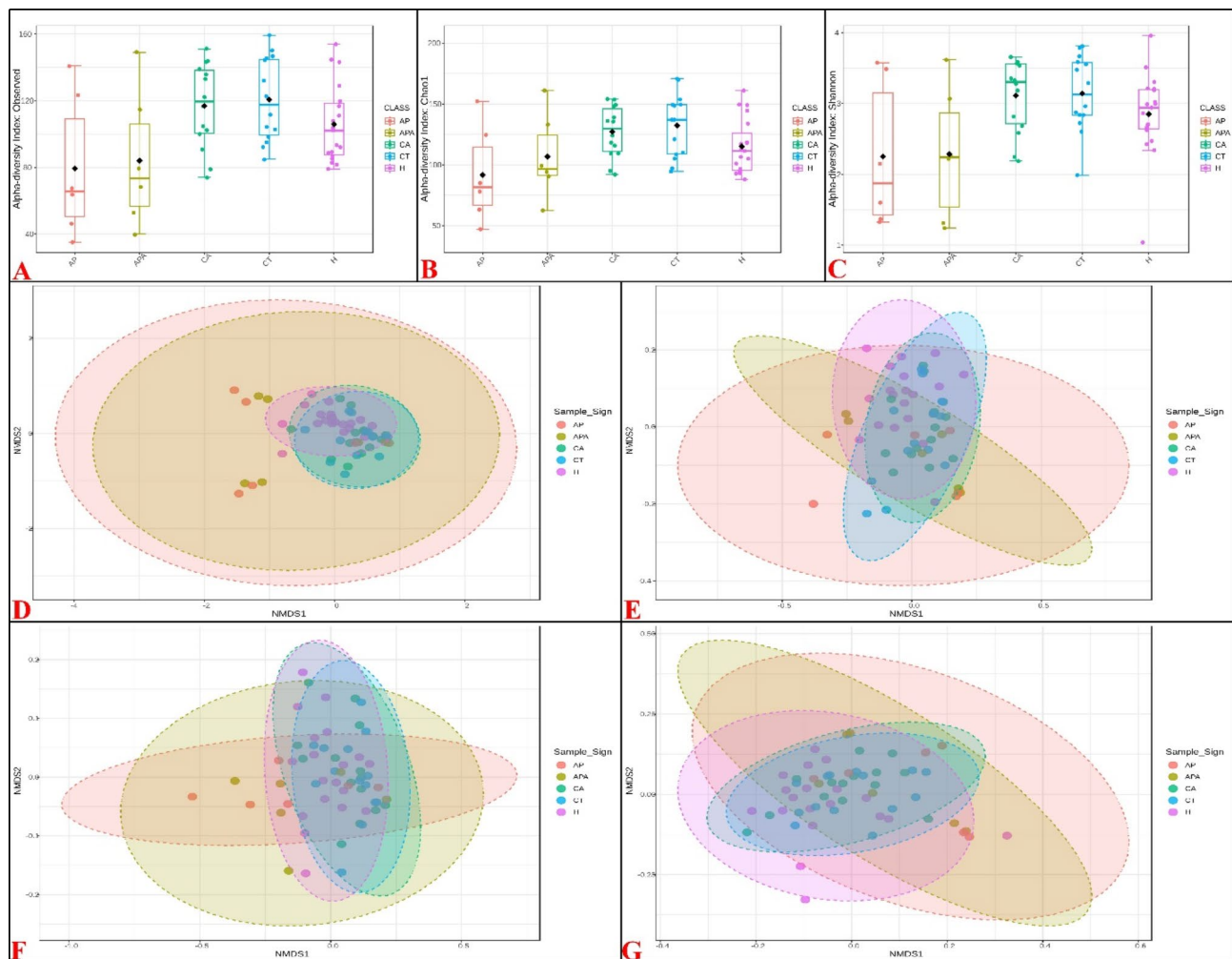


Fig. 3 Alpha and beta diversities of bacteriomes in studied groups. The figure indicates alpha and beta diversities of colorectal tissue bacteriome at the species level (H: healthy, CT: cancer tumor, CA: cancer tumor adjacent, AP: adenomatous polyps, and APA: adenomatous polyps adjacent). **(A)** alpha diversity of different studied groups using observed ESVs as diversity measure, and T-test / ANOVA as statistical method (p -value 0.010908; [ANOVA] F-value 3.6255). **(B)** alpha diversity of different studied groups using Chao1 index as diversity measure and T-test / ANOVA as the statistical method (p -value 0.01811; [ANOVA] F-value 3.2628). **(C)** alpha diversity of different studied groups using Shannon index as diversity measure and T-test / ANOVA as the statistical method (p -value 0.011059; [ANOVA] F-value 3.6156). **(D)** beta diversity using the ordination-based method of non-metric multidimensional scaling (NMDS), Bray-Curtis Index as distance method, and PERMANOVA (Permutational multivariate analysis of variance) as the statistical method ([PERMANOVA] F-value: 1.9149; p -value: 0.001). **(E)** beta diversity using the ordination-based method NMDS, Jensen-Shannon Divergence as the distance method, and PERMANOVA as the statistical method ([PERMANOVA] F-value: 2.2486; p -value: 0.001). **(F)** beta diversity using the ordination-based method NMDS Unweighted UniFrac as the distance method, and PERMANOVA as the statistical method ([PERMANOVA] F-value: 1.8716; p -value: 0.002). **(G)** beta diversity using the ordination-based method NMDS Weighted UniFrac as the distance method, and PERMANOVA as the statistical method ([PERMANOVA] F-value: 2.1332; p -value: 0.005)

family proportions were also decreased throughout APA, AP, CA, H, and CT groups (21.5%, 18.6%, 14.7%, 12.2%, and 11.6%, respectively). Bacteroidaceae, Lachnospiraceae, and Enterobacteriaceae were the most abundant families among the studied groups (30.3%, 19.7%, and 15.7%, respectively) (Fig. 4D).

Furthermore, to identify microbial taxa (including genera and species) that were significantly different between studied groups, statistical comparisons were done using Deseq2 as a statistical index and adjusted cutoff

p -value < 0.05. The results of significant genera and species were summarized in Table S5.

The Taxon Set Enrichment Analysis TSEA module built in the MicrobiomeAnalyst tool was used to detect the most frequent microbial taxa related to human pathologies and nosologies from a list of microbial features found in patients with CRC and healthy people [16]. The 5 top related diseases according to TSEA for H and CT groups were listed in Table S6. Four out of the top five related diseases in the CT group were CRC (global signature), colorectal carcinogenesis (carcinoma,



Fig. 4 Bacterial taxonomic composition of bacteriomes in different colorectal tissues (H: healthy, CT: cancer tumor, CA: cancer tumor adjacent, AP: adenomatous polyps, and APA: adenomatous polyps adjacent) in different taxonomic levels (phylum, class, order, family, genus, and species) represented by stacked bar plots. Stacked bar chart for relative abundance of the bacterial (A) phyla-level, (B) class-level, (C) order-level, (D) top 30 abundant families, (E) top 30 abundant genera, and (F) top 50 abundant species in different colorectal tissues. Features with counts smaller than 4 and 10% prevalence filtered as low read counts due to probable sequencing errors or low-level contamination. 10% of the features with the lowest percentages were also excluded using the inter-quartile range (IQR) as a low variance filter

increase), colorectal neoplasms (increase), and colorectal neoplasms (present). On the contrary, none of the first 5 top related diseases in the H group were related to the CRC (Fig. 5, Table S6).

Metabolites

An OPLS-DA was obtained from comparative analysis data between different studied groups to verify which metabolites were responsible for differentiating the samples from different groups including H versus CT,

H versus AP, and AP versus CT groups. The OPLS-DA score graphs (Fig. 6A and C) suggest that different studied groups had distinct groups of metabolites. The values of model validation with permutation tests (2000 permutations) for H vs. CT groups ([R2Y:0.749, p: 0.0085], [Q2:0.593, p<0.0005]), H vs. AP groups ([R2Y:0.987, p: 0.0085], [Q2:0.827, p:0.002]) were satisfactory, suggesting a statistically significant difference between the metabolic profiles of the studied groups analyzed. In the AP versus CT groups, the values of model validation with

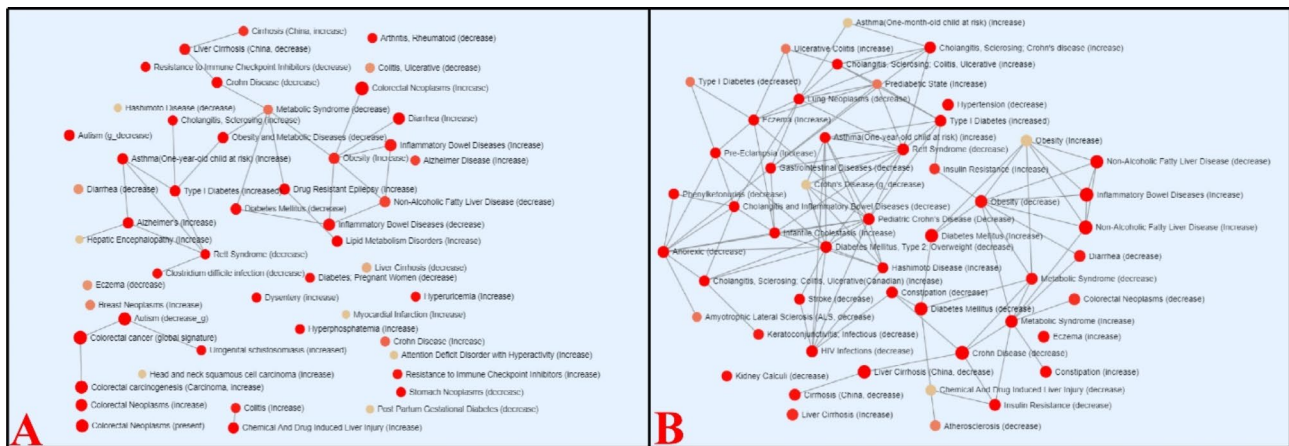


Fig. 5 The TSEA (Taxon Set Enrichment Analysis) module. **(A)** TSEA results using the most prevalent genera and species revealed in bacteriomes of CRC patients' colorectal tissues. **(B)** TSEA results using the most prevalent genera and species revealed in bacteriomes of healthy individual's colorectal tissues. Each node represents a taxon set with its color based on its *p*-value, and its size is based on the number of hits to the query. An edge connects two taxon sets if the shared hits exceed 20% of their combined taxa

permutation tests (2000 permutations) ([R2Y:0.869, *p*:0.137], [Q2: -0.222, *p*:0.4185) were not satisfactory, suggesting a statistically insignificant difference between the metabolic profiles of these studied groups (Fig. 6D and F). The VIP value was employed for metabolite selection using each metabolite loading weight and variability of the response, to differentiate studied groups from each other. The *x*-axis in the VIP plots shows the value of VIP. Metabolite with high VIP has more contribution in the group separation (Fig. 6G and I). Advanced significance analysis such as significant analysis of metabolites (SAM) allowed us to illustrate different study group's metabolite changes (i.e., increased or decreased) in comparison to each other. Applying SAM, we identified 5 metabolites that significantly increased in the CT group tissues in comparison to the H group tissues (BHB, acetoacetate, acetate, leucine, and fumarate). When comparing the H group with the AP group, we identified 5 metabolites significantly different in the two groups, three of them decreased in the AP group (phosphocholine, phosphocreatine, and myo-inositol), and two of them increased (acetoacetate and BHB) in the AP group (Fig. 6J and L).

Bacteriome-metabolome associations

To investigate the associations among the colorectal tissue bacteriome and metabolites, the Distance correlation test was employed to evaluate the associations between the identified bacterial species and metabolites according to their relative abundances (Fig. 7). The correlations among the differential colorectal tissue metabolites and altered bacterial species were summarized in Table S7. Significant associations were observed between species in colorectal bacteriomes and metabolites comparing different groups (H compared to AP [Fig. 7A], and H compared to CT [Fig. 7B]). When comparing the AP group with the

H group, we observed a significant correlation between the increase of both acetoacetate and beta-hydroxybutyric acid (BHB) and a decrease in the abundances of 17 species mostly belonging to the Lachnospiraceae family in the AP group. Additionally, our results revealed correlations in a decrease of both phosphocholine/choline concentration and relative abundances of *Lachnospira rogosa* and *Choladocola sp018223365* in the AP group. On the other hand, when comparing bacteriome-metabolome associations in the CT and H groups, we found significant correlations between the increase of fumarate and high relative abundances of *Aeromonas enteropelogenes*, *Aeromonas veronii*, and *Fusobacterium nucleatum* subsp. *animalis* in the CT tissues. Moreover, *CAG 269 sp017458285*, *Prevotella sp900551275*, and *Scatomorpha sp900752445* increase were associated with an increase of acetate. In the same way, the relative abundance of *Anaerostignum faecicola* and acetoacetate concentration were increased simultaneously and significantly in the CT tissues. On the contrary, the decrease of the *Choladocola sp018223365* relative abundance correlated with BHB increase in the CT group.

Discussion

With the importance of CRC bacteriome and metabolome in mind, we investigated the bacterial and metabolite composition of the different study group's mucosal tissues. We observed a significant decrease of colorectal bacteriome alpha diversity metrics throughout CT, CA, H, APA, and AP groups, respectively, suggesting that bacteriome richness and evenness significantly decrease in the precancerous tissues whereas they sharply increase in the cancer tissues when compared to healthy samples. In the same way, some researchers concluded that mucosal bacterial composition in the cancer group was richer

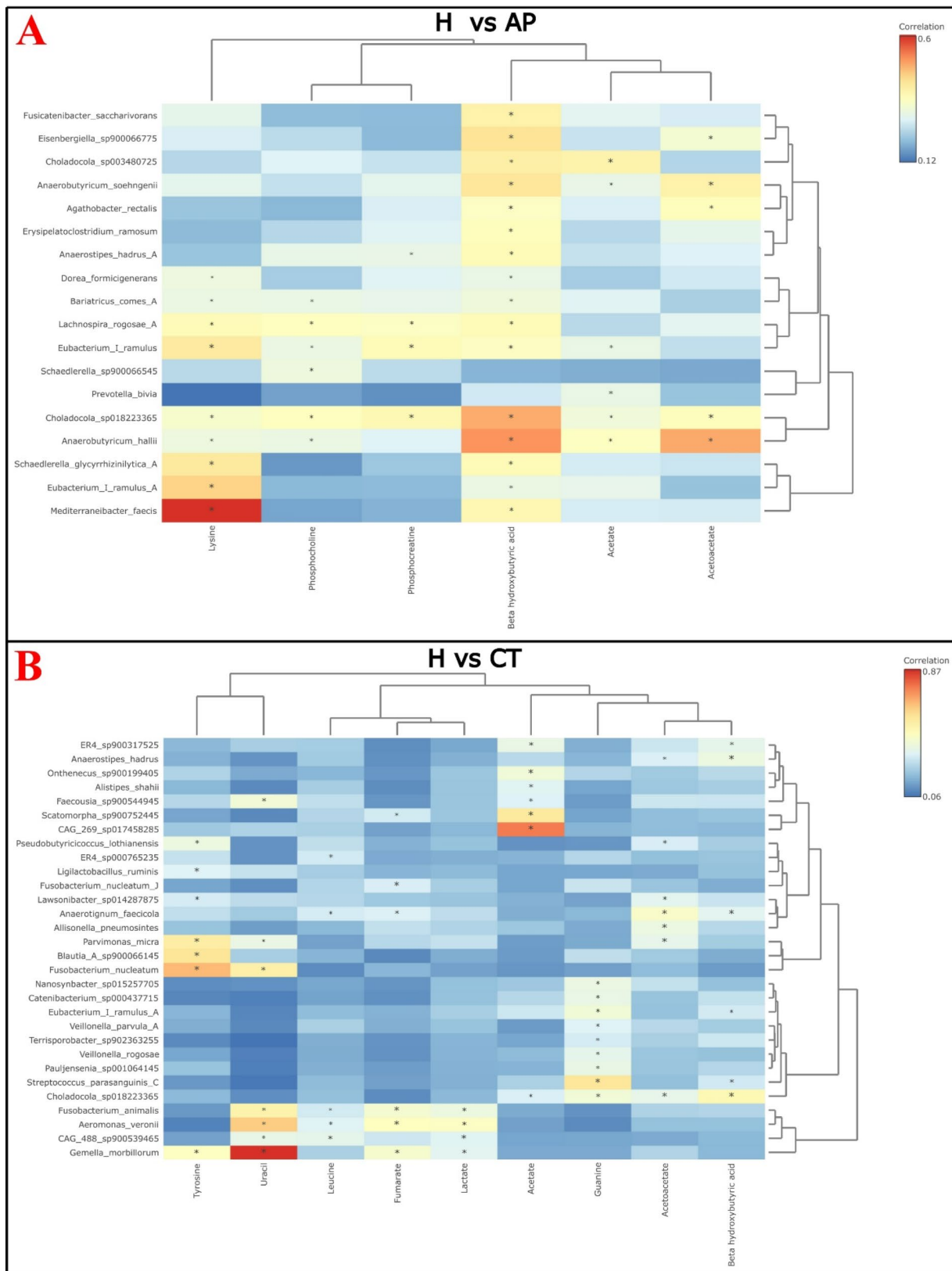


Fig. 7 (See legend on next page.)

(See figure on previous page.)

Fig. 7 Correlation heatmap of colorectal bacteriome metabolome using Distance correlation test as similarity method. 10% of reads were removed as variance filter based on inter-quartile range, reads with counts less than 4 were also removed as abundance filter. Data scaled via autoscaling as normalization. Different studied groups were used as primary metadata (fixed effects). Age, BMI, and sex of the participants were used as covariates and accounted for in the statistics extracted for the primary metadata. MaAsLine2 is used for microbiome comparison analysis and Limma is used for metabolomics data. Features with a p -value less than 0.01 were considered significant. Significant correlations are highlighted with asterisks. The correlation threshold was set to more than 0.35. The color indicates the correlation calculated by the distance test as a similarity method. Comparisons were done between the healthy (H) vs. adenomatous polyp (AP) group (**A**), and the H vs. cancer tumor (CT) group (**B**) at the species taxonomic level with their identified metabolites according to their relative abundances

than in the healthy group tissues [20, 21]. However, this is in contrast to other studies which found that the microbial diversity of CRC patients was significantly lower than that of the healthy controls [22]. It is noteworthy to state that they compared tumor tissues with off-tumor normal tissues of the same individuals as healthy controls which had shown to have similar alpha diversities in other research [23]. On the other hand, we found that there are significant differences in beta diversity when comparing H with CT, CA, AP, and APA groups. Likewise, other researchers showed that there are distinct patterns of bacterial distribution among the H, CT, and AP groups [24].

Firmicutes and Bacteroidetes are the two most dominant bacterial phyla in the human gut bacteriome representing more than 90% of bacterial total composition [25]. Although some researchers concluded that the F/B ratio has crucial effects on normal intestinal homeostasis [26], other studies suggested that it is presently delicate to associate the F/B ratio with certain health status [25]. Our results propose that low F/B ratios may be associated with CRC initiation and development. In the same way, it was hypothesized that the downregulated F/B ratio in colorectal tissues of CRC patients may affect the tumorigenesis process [27]. Concerning the phyla level, our results showed that the proportion of Fusobacteria significantly increased in AP and CT groups when compared to the H group suggesting its proposed role in the carcinogenesis initiation and progression. Similarly, some studies concluded that there was an increasing trend of Fusobacteria with the CRC progression [28]. On the other hand, our results showed that Campylobacterota was only present in the CT group suggesting its contribution as a secondary passenger in the cancer progression. Recently, some researchers proposed the association of Campylobacterota with intestinal diseases like ulcerative colitis [29]. In addition, we found that there was a significant increase in Proteobacteria in the AP group when compared with the H and CT groups indicating its proposed role in cancer initiation. Likewise, other researchers observed that there was a significantly higher abundance of Proteobacteria in adenoma polyps compared to the non-adenoma group [30]. Moreover, we showed that Patescibacteria was significantly increased in the H group compared to the AP group. Patescibacteria (also known as candidate phyla

radiation), is an emerging, uncultured, and ubiquitous superphylum that can sometimes be found within the human microbiome like the human mouth, lungs, and gut [31]. Other researchers indicated that Patescibacteria was significantly represented in the gut microbiome of a healthy adult population [32]. Since Patescibacteria have a range of free-living, episymbiotic, parasitic, and predatory life cycles, they may be able to modulate the gut bacteriome directly or indirectly by changing the composition of other dominant phyla [33]. In the same way, it was shown that Saccharibacteria (a member of Patescibacteria) might prevent bacterial-induced inflammation in the host mammalians [34].

Concerning the genus level, when comparing the AP with the H group, our results showed that there are significantly enriched genera in the AP group some of which were *Morganella*, *Gemella*, and *Escherichia*. In the same way, other researchers showed that *Morganella* [35], *Gemella* [11], and *Escherichia* [36] were significantly increased in the adenomatous polyps compared to the healthy samples indicating their proposed driver role in the cancer initiation in precancerous microenvironments. Moreover, there were significantly enriched genera in the CT group compared to the H group some of which were *Fusobacterium*, *Parvimonas*, *Aeromonas*, *Campylobacter*, *Anaerotignum*, and *Gemella*. In parallel, other researchers showed that *Fusobacterium* [37], *Parvimonas* [23], *Campylobacter* [38], and *Anaerotignum* [39] had increased abundance in the cancer group compared to the healthy group. These two significant consortia of bacterial genera are completely different except for the *Gemella* genus indicating that there are distinct bacterial groups involved in the cancer initiation and progression inside the precancerous and cancerous microenvironments. Even though abundance of *Gemella* increased in the CT group when compared to the H group similar to the other research that identified the *Gemella* genus as a non-invasive biomarker for CRC [40], our results in parallel to other studies [11] showed that the *Gemella* genus was more prevalent in the AP group compared to the CT group indicating that the development of a malignancy-related bacteriome including *Gemella morbillorum* appears before tumor establishment [41].

Interestingly, when we compared the AP group with the CT group, we observed a significant rise of *Campylobacter sp.*, *A. enteropelogenes*, *F. nucleatum* subsp.

nucleatum, *Bacteroides fragilis*, *F. nucleatum* subsp. *animalis*, *Streptococcus* sp., and *Parvimonas micra* in the CT group, as well as a significant reduction of *Prevotella bivia*, *G. morbillorum*, *Morganella* sp., *Veillonella parvula*, *Bacteroides clarus*, and *Ruminococcus gnavus*. In the same way, some researchers concluded that the mucosal and fecal microbial profiles of CRC patients are different from those of AP patients [11]. On the other hand, it was shown that the *Fusobacterium* genus in the stool samples was significantly associated with CRC compared to individuals with adenomas indicating that *Fusobacterium* is more likely a passenger multiplying in suitable situations of CRC than a causal driver in the AP group to establish a cancerous condition [37]. Moreover, other studies showed that *Fusobacterium* spp. and Enterotoxigenic *Bacteroides fragilis* (ETBF) had higher proportions in the late stages of CRC compared to the early stages demonstrating their proposed carcinogenic contribution after a primary carcinogenic hit [42]. In addition, similar to our results, *Campylobacter* sp. [43], *A. enteropelogenes* [44], and *P. micra* [45] were shown to be enriched and used as discrimination biomarkers of CRC from adenoma polyps.

On the other hand, in agreement with our results, the proportion of *Morganella* spp. was shown to increase in bacteriomes of the primary gastrointestinal tumors and caused colon tumorigenesis producing different genotoxic metabolites [46]. Similarly, other researchers indicated that even though *Prevotella* species were not cytotoxic or inflammatory, these bacteria were able to change the barrier features of the epithelium and finally affect the colonization of secondary colonizers [47]. In the same way, *V. parvula* has been shown to increase in adenoma patients [48] and modulates its metabolic condition to colonize the intestine during inflammation [49]. Additionally, similar to our results, some researchers showed that *R. gnavus* abundance significantly increased in adenoma polyp mucosal tissues suggesting that polyp microenvironments are inflammatory niches containing distinct bacterial groups [36]. Although some researchers identified *G. morbillorum* as a potential non-invasive biomarker for colorectal cancer [40], some other researchers concluded that the development of a malignancy-related bacteriome including *G. morbillorum* appears before tumor establishment [41]. Consequently, our TSEA results of significantly changing bacteria within the CT and H groups also confirmed that CT-related bacteriome had a strong correlation with increased CRC in humans validating our bacterial changes associated with colorectal cancer (Fig. 5, Table S6).

Bacterial metabolites could lead to TME metabolic activity and ecological composition reconstruction resulting in cancer stimulation [8]. In the same way, we observed significantly distinct extracted metabolites

from mucosal samples of different groups. Five metabolites significantly increased in the CT group compared to the H group including BHB, acetoacetate, acetate, leucine, and fumarate. In the same way, other studies showed that there was an accumulation of BHB, acetoacetate, and acetate in the mucosal samples of rectal cancer compared to healthy tissues [15] indicating an altered energy metabolism in the inflammatory conditions [50]. Increased amounts of acetate might propose its role as a metabolic fuel for ATP supply in CRC [51]. Leucine is one of the branched-chain amino acids (BCAAs). Some researchers showed that BCAA catabolism loss and its consequent enrichment activates mTORC1 and thus leads to tumor progression [52]. Furthermore, it has been shown that fumarate accumulation in tumors leads to carcinogenic pathway activation [53] and it is a metabolic barrier to anti-tumor features of CD8⁺ T cells in the TME [54].

Interestingly, our results showed that two metabolites increased in the AP group compared to the H group including BHB and acetoacetate, whereas three metabolites decreased in the AP group compared to the H group including phosphocholine, phosphocreatine, and myo-inositol. In the same line, a meta-analysis showed that there was a significant increase of choline TMA-lyase encoding gene (*cutC*), one of the genes belonging to the main trimethylamine synthesis pathways, in bacteriomes of adenoma and CRC patients compared to healthy samples [55] proposing the reason of decreased amounts of choline and increased amounts of trimethylamine-N-oxide in our AP samples compared to the H group. In addition, other studies concluded that gut microbial utilized colonic creatine and phosphocreatine can influence gut pathology and physiology by improving the epithelial barrier function [56]. Moreover, other studies showed that tissue and cellular levels of inositol decreased in the polyp tissue compared to healthy tissues in the APC^{min/+} mice, which suffer from polyps similar to human familial adenomatous polyposis [57]. Some other researchers proposed that myo-inositol might prevent carcinogenesis and its administration also decreased the size of adenocarcinoma [58].

CRC initiation and progression are strictly associated with both the bacteriome and metabolome and their potential interconnections [38]. Similarly, when comparing bacteriome and metabolome correlations between groups AP and H, our results showed that increased concentrations of acetoacetate and BHB had a significant correlation with a decrease in relative abundance for several species belonging to the Lachnospiraceae family. Similarly, other researchers showed that most members of the Lachnospiraceae family decreased during colorectal cancer [59, 60]. The Lachnospiraceae family members are present in most individual gut core bacteriomes and

occupy a large proportion of the total potentially butyrate-producing bacteria [61]. On the other hand, BHB and acetoacetate as ketone bodies are proposed to be involved in cancer prevention [62] and decreased in CRC patients [63]. On the contrary, our results showed that BHB and acetoacetate were increased in the tissue samples of the AP and CT groups compared to the H group. In parallel, other researchers concluded that as a result of the Warburg effect, glucose is used as fuel by colon cancer cells instead of SCFA resulting in the dominance of glycolytic metabolism over oxidative phosphorylation in malignant colonocytes, which finally leads to butyrate and its downstream products (including acetoacetate and BHB) accumulation [64]. In addition, it was shown that mammalian crypt structures protect stem/progenitor growth in part through a metabolic barrier created by butyrate-feeding differentiated colonocytes. Probable crypt destruction due to CRC or adenomatous polyps may cause increased exposure of butyrate to the stem/progenitor cells which may result in proliferation inhibition [65]. Moreover, our results showed that choline (or its phosphorylated form) decreased in the precancerous AP group. In the same way, some researchers concluded that choline metabolism dysregulation has a critical role in cancer initiation [66]. Moreover, other researchers found that there is an increased concentration of choline TMA-lyase (*cutC*) in CRC samples compared to controls. They also identified some unknown species that had the most prevalent *cutC* sequence and were placed within the Lachnospiraceae family [55].

When comparing bacteriome and metabolome correlations between groups CT and H, our results showed that BHB increase was related significantly to the depletion of the *Choladocola sp018223365*. Acetoacetate enrichment was related to the *Anaerotignum faecicola* increased abundance in the CT group in our results. Similarly, other researchers showed that *Anaerotignum sp.* was enriched in the cancer group [39]. In addition, higher concentrations of acetate were significantly related to an increased abundance of *CAG 269 sp017458285*, *Prevotella sp900551275*, and *Scatomorpha sp900752445*. In the same way, some researchers showed that a level of *CAG 269 sp.* significantly decreased in individuals recovered from ulcerative colitis (UC) compared to samples with UC at the active stage indicating the probable relationship of the *CAG 269 sp.* with chronic intestinal inflammatory diseases [67]. Furthermore, our results showed that fumarate increase in the CT group was significantly related to the *A. enteropelogenes*, *A. veronii*, and *F. animalis* higher abundances. Microbial metabolites like fumarate can be enriched within the TME and be involved in carcinogenesis. Some researchers showed that *F. nucleatum* produces succinate (that can be converted to fumarate bidirectionally) facilitating

CRC development [68]. In the same way, other researchers showed that *Aeromonas* infection leads to succinate accumulation [69].

Keeping our interesting findings on one hand, our study had some limitations like a relatively small sample size of 60 tissue samples on the other hand. Even though collecting biopsies during primary endoscopy from individuals without medical alterations is of great value, we should acknowledge that alternative larger cohorts are needed to validate further our findings.

Conclusion

In light of our research findings, we demonstrated that there are distinct bacteriomes and metabolomes present in CRC TMEs, precancerous polyps, and healthy individuals' gut tissues. Our results indicated that bacterial richness and evenness in colorectal tissues are significantly lower before cancer initiation (adenomatous polyps) including depletion in healthy gut-beneficial bacteria like Lachnospiraceae family members in concordance with beta-hydroxybutyric acid and acetoacetate accumulation in the polyp microenvironments. Moreover, our results suggest that some driver bacteria accumulation including *Gemella morbillorum*, and *Morganella morganii* in precancerous polyps, and increased abundance of passenger bacterial species like *Anaerotignum faecicola*, *CAG 269 sp.*, *Prevotella sp.*, and *Scatomorpha sp.*, *Aeromonas enteropelogenes*, *Aeromonas veronii*, and *Fusobacterium nucleatum* subsp. *animalis* in concurrence with acetoacetate, acetate, and fumarate accumulation within the TMEs might have important roles in colorectal cancer initiation and progression procedure, respectively. While healthy gut bacteriome and metabolome can prevent malignancies, bacterial and metabolite composition in precancerous adenomatous polyps can be used in early CRC diagnosis. In addition, CRC TME composition can be used in preventing cancer progression, designing novel treatment methods, and therefore achieving good prognosis. Further research and confirmation of these findings in larger sample sizes would be useful to develop metabolome and bacteriome-based preventive, diagnostic, and treatment approaches for CRC.

Abbreviations

CRC	Colorectal cancer
TME	Tumor microenvironment
H	Healthy
AP	Adenomatous polyps
APA	Adenomatous polyps-adjacent
CT	Cancer tumor
CA	Cancer tumor-adjacent
EOCRC	Early-onset colorectal cancer
OPLS-DA	Orthogonal partial least squares-discriminant analysis
SAM	Significant analysis of metabolites
ESV	Exact sequence variants
NMDS	Non-metric multidimensional scaling
TSEA	Taxon Set Enrichment Analysis
DESeq2	Differential expression analysis for sequence count data v. 2

IQR	Inter-quantile range
BHB	Beta-hydroxybutyric acid
PERMANOVA	Permutational multivariate analysis of variance
VIP	Variable importance in projection
BCAA	Branched-chain amino acid
UC	Ulcerative colitis
FDR	False discovery rate

Supplementary Information

The online version contains supplementary material available at <https://doi.org/10.1186/s12941-025-00777-9>.

Supplementary Material 1

Acknowledgements

We appreciate the study participants for their contribution to this research. We are also grateful to Dr. Seyed Kazem Forghani for his valuable histopathology consultation about tissue samples. We acknowledge Sanaz Sajedi-Amin for her assistance in metabolic data interpretation.

Author contributions

H.F. designed and performed the experiments, derived the models and analyzed the data, drafted the manuscript, and designed the figures. H.S.K. designed the experiments and supervised the project. M.A.R. was involved in planning and supervising the work. A.P. and V.K. and A.B. and E.F. conducted the isolation of DNA, preparation, and sequencing of DNA libraries. R.G. is involved in planning and supervising the work. M.S. contributed to sample preparation. H.K. aided in interpreting the results and worked on the manuscript. F.S.K. and S.N. performed the HNMR and analyzed spectra. All authors read and approved the final manuscript.

Funding

This study was supported by the Drug Applied Research Center, Tabriz University of Medical Sciences with grant number 65967.

Data availability

All data generated and/or analyzed during the current study have been provided throughout the text, in the supplementary tables, or are publicly available in GitHub (https://github.com/FLR-ASB/CRC_microbiome), and NCBI Sequence Read Archive (SRA) database, (<http://www.ncbi.nlm.nih.gov/bioproject/1138929>) with BioProject accession number PRJNA1138929.

Declarations

Ethics approval and consent to participate

The protocols described in this document were approved by the Tabriz Regional Ethics Committee (Tabriz University of Medical Sciences, Tabriz, Iran), No. I.R.TBZMED.REC.1400.155. All the procedures were done according to the Helsinki Declaration, and informed consent was obtained from all participants.

Competing interests

The authors declare no competing interests.

Consent for publication

All authors declare agreement and consent for publication.

Author details

¹Drug Applied Research Center, Faculty of Medicine, Tabriz University of Medical Sciences, Tabriz, Iran

²Department of Medical Microbiology, Aalinasab Hospital, Social Security Organization, Tabriz, Iran

³Institute for Cellular and Intracellular Symbiosis of the Ural Branch of the Russian Academy of Sciences, Orenburg, Russia

⁴Department of Bacteriology and Virology, Faculty of Medicine, Tabriz University of Medical Sciences, Tabriz, Iran

⁵Department of Internal Medicine, Tabriz Branch, Islamic Azad University, Tabriz, Iran

⁶Department of Chemistry, University of Copenhagen, Copenhagen, Denmark

⁷Department of Science and Environment, Roskilde University, Roskilde, Denmark

⁸Mahabad Faculty of Medical Sciences, Urmia University of Medical Sciences, Urmia, Iran

Received: 7 December 2024 / Accepted: 20 January 2025

Published online: 29 January 2025

References

1. Bray F, Laversanne M, Sung H, Ferlay J, Siegel RL, Soerjomataram I, Jemal A. Global cancer statistics 2022: GLOBOCAN estimates of incidence and mortality worldwide for 36 cancers in 185 countries. *Cancer J Clin*. 2022;74(3):229–63.
2. Feizi H, Plotnikov A, Rezaee MA, Ganbarov K, Kamounah FS, Nikitin S, Kadkhoda H, Gholizadeh P, Pagliano P, Kafil HS. Postbiotics versus probiotics in early-onset colorectal cancer. *Crit Rev Food Sci Nutr*. 2024;64(11):3573–82.
3. Feizi H, Rezaee AM, Ghotaslou R, Sadrkabir M, Jadidi-Niaragh F, Gholizadeh P, Taghizadeh S, Ghanbarov K, Yousefi M, Kafil SH. Gut microbiota and colorectal Cancer risk factors. *Curr Pharm Biotechnol*. 2023;24(8):1018–34.
4. White MT, Sears CL. The microbial landscape of colorectal cancer. *Nat Rev Microbiol*. 2024;22(4):240–54.
5. Rezasoltani S, Azizmohammad Looha M, Asadzadeh Aghdaei H, Jasemi S, Sechi LA, Gazouli M, Sadeghi A, Torkashvand S, Baniali R, Schlüter H, et al. 16S rRNA sequencing analysis of the oral and fecal microbiota in colorectal cancer positives versus colorectal cancer negatives in Iranian population. *Gut Pathogens*. 2024;16(1):9.
6. Zhang M, Lv Y, Hou S, Liu Y, Wang Y, Wan X. Differential Mucosal Microbiome profiles across stages of Human Colorectal Cancer. *Life*. 2021;11(8):831.
7. Nenkov M, Ma Y, Gaßler N, Chen Y. Metabolic reprogramming of Colorectal Cancer cells and the Microenvironment: implication for Therapy. *Int J Mol Sci*. 2021;22(12):6262.
8. Zhang W, An Y, Qin X, Wu X, Wang X, Hou H, Song X, Liu T, Wang B, Huang X et al. Gut microbiota-derived metabolites in Colorectal Cancer: the bad and the challenges. *Front Oncol* 2021, 11.
9. Kim M, Vogtmann E, Ahlquist DA, Devens ME, Kiesel JB, Taylor WR, White BA, Hale VL, Sung J, Chia N, et al. Fecal metabolomic signatures in colorectal adenoma patients are Associated with Gut Microbiota and early events of Colorectal Cancer Pathogenesis. *mBio*. 2020;11(1). <https://doi.org/10.1128/mBio.03186-03119>.
10. Tang Q, Jin G, Wang G, Liu T, Liu X, Wang B, Cao H. Current sampling methods for gut microbiota: a call for more precise devices. *Front Cell Infect Microbiol*. 2020;10:151.
11. Russo E, Gloria LD, Nannini G, Meoni G, Niccolai E, Ringressi MN, Baldi S, Fani R, Tenori L, Taddei A, et al. From adenoma to CRC stages: the oral-gut microbiome axis as a source of potential microbial and metabolic biomarkers of malignancy. *Neoplasia*. 2023;40:100901.
12. Tsigalou C, Paraschaki A, Bragazzi NL, Aftzoglou K, Stavropoulou E, Tsakris Z, Vradelis S, Bezirtzoglou E. Alterations of gut microbiome following gastrointestinal surgical procedures and their potential complications. *Front Cell Infect Microbiol* 2023, 13.
13. Kim D, Jung JY, Oh HS, Jee SR, Park SJ, Lee SH, Yoon JS, Yu SJ, Yoon IC, Lee HS. Comparison of sampling methods in assessing the microbiome from patients with ulcerative colitis. *BMC Gastroenterol*. 2021;21(1):396.
14. Lee-Sarwar KA, Lasky-Su J, Kelly RS, Litonjua AA, Weiss ST. Metabolome-Microbiome Crosstalk and Human Disease. *Metabolites* 2020, 10(5).
15. Wang H, Wang L, Zhang H, Deng P, Chen J, Zhou B, Hu J, Zou J, Lu W, Xiang P, et al. ¹H NMR-based metabolic profiling of human rectal cancer tissue. *Mol Cancer*. 2013;12(1):121.
16. Lu Y, Zhou G, Ewald J, Pang Z, Shiri T, Xia J. MicrobiomeAnalyst 2.0: comprehensive statistical, functional and integrative analysis of microbiome data. *Nucleic Acids Res*. 2023;51(W1):W310–8.
17. Edgar RC, Flyvbjerg H. Error filtering, pair assembly and error correction for next-generation sequencing reads. *Bioinformatics*. 2015;31(21):3476–82.
18. Parks DH, Chuvochina M, Rinke C, Mussig AJ, Chaumeil P-A, Hugenholtz P. GTDB: an ongoing census of bacterial and archaeal diversity through a phylogenetically consistent, rank normalized and complete genome-based taxonomy. *Nucleic Acids Res*. 2022;50(D1):D785–94.
19. Love MI, Huber W, Anders S. Moderated estimation of Fold change and dispersion for RNA-seq data with DESeq2. *Genome Biol*. 2014;15:1–21.

20. Abdi H, Kordi-Tamandani DM, Lagzian M, Bakhsipour A. Composition and diversity differences between Colon microbiome of Colorectal Cancer patients and healthy individuals by Age. *J Epigenetics*. 2021;2(2):45–50.
21. Thomas AM, Jesus EC, Lopes A, Aguiar S Jr, Begnami MD, Rocha RM, Carpinetti PA, Camargo AA, Hoffmann C, Freitas HC, et al. Tissue-Associated bacterial alterations in rectal carcinoma patients revealed by 16S rRNA community profiling. *Front Cell Infect Microbiol*. 2016;6:179.
22. Choi S, Chung J, Cho M-L, Park D, Choi SS. Analysis of changes in microbiome compositions related to the prognosis of colorectal cancer patients based on tissue-derived 16S rRNA sequences. *J Translational Med*. 2021;19(1):485.
23. Flemer B, Lynch DB, Brown JM, Jeffery IB, Ryan FJ, Claesson MJ, O'Riordain M, Shanahan F, O'Toole PW. Tumour-associated and non-tumour-associated microbiota in colorectal cancer. *Cut*. 2017;66(4):633–43.
24. Grion BAR, Fonseca PLC, Kato RB, Garcia GJY, Vaz ABM, Jiménez BN, Dambolena AL, Garcia-Etxebarria K, Brenig B, Azevedo V et al. Identification of taxonomic changes in the fecal bacteriome associated with colorectal polyps and cancer: potential biomarkers for early diagnosis. *Front Microbiol* 2024, 14.
25. Magne F, Gotteland M, Gauthier L, Zazueta A, Pesoa S, Navarrete P, Balamurugan R. The Firmicutes/Bacteroidetes ratio: a relevant marker of gut dysbiosis in obese patients? *Nutrients* 2020, 12(5):1474.
26. Stojanov S, Berlec A, Štrukelj B. The influence of Probiotics on the Firmicutes/Bacteroidetes ratio in the Treatment of Obesity and inflammatory bowel disease. *Microorganisms* 2020, 8(11).
27. Xu Y, Zhao J, Ma Y, Liu J, Cui Y, Yuan Y, Xiang C, Ma D, Liu H. The microbiome types of colorectal tissue are potentially associated with the prognosis of patients with colorectal cancer. *Front Microbiol* 2023, 14.
28. Zhao L, Grimes SM, Greer SU, Kubit M, Lee H, Nadauld Lincoln D, Ji HanLee P. Characterization of the consensus mucosal microbiome of colorectal cancer. *NAR Cancer* 2021, 3(4).
29. Shao J, Li Z, Gao Y, Zhao K, Lin M, Li Y, Wang S, Liu Y, Chen L. Construction of a bacteria-metabolites co-expression network to clarify the anti-ulcerative colitis effect of flavonoids of *Sophora flavescens* Aiton by regulating the host-microbe interaction. *Front Pharmacol*. 2021;12:710052.
30. Sanapareddy N, Legge RM, Jovov B, McCoy A, Burcal L, Araujo-Perez F, Randall TA, Galanko J, Benson A, Sandler RS. Increased rectal microbial richness is associated with the presence of colorectal adenomas in humans. *ISME J*. 2012;6(10):1858–68.
31. Castelle CJ, Brown CT, Anantharaman K, Probst AJ, Huang RH, Banfield JF. Biosynthetic capacity, metabolic variety and unusual biology in the CPR and DPANN radiations. *Nat Rev Microbiol*. 2018;16(10):629–45.
32. Latorre-Pérez A, Hernández M, Iglesias JR, Morán J, Pascual J, Porcar M, Vilanova C, Collado L. The Spanish gut microbiome reveals links between microorganisms and Mediterranean diet. *Sci Rep*. 2021;11(1):21602.
33. Vigneron A, Cruaud P, Guyoneaud R, Goñi-Urriza M. Into the darkness of the microbial dark matter in situ activities through expression profiles of Patesci-bacteria populations. *Front Microbiol* 2023, 13.
34. Chipashvili O, Utter DR, Bedree JK, Ma Y, Schulte F, Mascarin G, Alayyoubi Y, Chouhan D, Hardt M, Bidlack F, et al. Epibiotic Saccharibacteria suppresses gingival inflammation and bone loss in mice through host bacterial modulation. *Cell Host Microbe*. 2021;29(11):1649–e16621647.
35. Wang YX, Huang HB, Dong YH, Li ZS, Liu F, Du YQ. Alterations and clinical relevance of gut microbiota in patients with Peutz-Jeghers syndrome: a prospective study. *J Dig Dis*. 2023;24(3):203–12.
36. Welham Z, Li J, Engel AF, Molloy MP. Mucosal Microbiome in Patients with Early Bowel Polyps: Inferences from Short-Read and Long-Read 16S rRNA Sequencing. *Cancers* 2023, 15(20):5045.
37. Amitay E, Werner S, Vital M, Pieper DH, Höfler D, Gierse I-J, Butt J, Balavara Y, Cuk K, Brenner H. Fusobacterium and colorectal cancer: causal factor or passenger? Results from a large colorectal cancer screening study. *Carcinogenesis*. 2017;38(8):781–8.
38. Feng K, Ren F, Wang X. Association between oral microbiome and seven types of cancers in east Asian population: a two-sample mendelian randomization analysis. *Front Mol Biosci* 2023, 10.
39. Liu C, Li Z, Ding J, Zhen H, Fang M, Nie C. Species-level analysis of the human gut Microbiome shows antibiotic resistance genes Associated with Colorectal Cancer. *Front Microbiol* 2021, 12.
40. Yao Y, Ni H, Wang X, Xu Q, Zhang J, Jiang L, Wang B, Song S, Zhu X. A new biomarker of fecal Bacteria for non-invasive diagnosis of Colorectal Cancer. *Front Cell Infect Microbiol*. 2021;11:744049.
41. Senthakumaran T, Moen AEF, Tannæs TM, Endres A, Brackmann SA, Rounge TB, Bemanian V, Tunsjø HS. Microbial dynamics with CRC progression: a study of the mucosal microbiota at multiple sites in cancers, adenomatous polyps, and healthy controls. *Eur J Clin Microbiol Infect Dis*. 2023;42(3):305–22.
42. Vijoen KS, Dakshinamurthy A, Goldberg P, Blackburn JM. Quantitative profiling of Colorectal Cancer-Associated Bacteria reveals associations between *Fusobacterium* spp., Enterotoxigenic *Bacteroides fragilis* (ETBF) and clinicopathological features of Colorectal Cancer. *PLoS ONE*. 2015;10(3):e0119462.
43. Wang J, Gao F, Li J, Zhang J, Li S, Xu GT, Xu L, Chen J, Lu L. The usability of WeChat as a mobile and interactive medium in student-centered medical teaching. *Biochem Mol Biol Educ*. 2017;45(5):421–5.
44. Sahankumari A, Gamage BD, Malavige GN. Association of the gut microbiota with colorectal cancer in a south Asian cohort of patients. *bioRxiv* 2019:694125.
45. Xu J, Yang M, Wang D, Zhang S, Yan S, Zhu Y, Chen W. Alteration of the abundance of Parvimonas micra in the gut along the adenoma-carcinoma sequence. *Oncol Lett*. 2020;20(4):1–1.
46. Cao Y, Oh J, Xue M, Huh WJ, Wang J, Gonzalez-Hernandez JA, Rice TA, Martin AL, Song D, Crawford JM. Commensal microbiota from patients with inflammatory bowel disease produce genotoxic metabolites. *Science*. 2022;378(6618):eabm3233.
47. İlhan ZE, Łaniewski P, Tonachio A, Herbst-Kralovetz MM. Members of Prevotella Genus distinctively modulate Innate Immune and Barrier functions in a human three-dimensional endometrial epithelial cell model. *J Infect Dis*. 2020;222(12):2082–92.
48. Wu Y, Jiao N, Zhu R, Zhang Y, Wu D, Wang A-J, Fang S, Tao L, Li Y, Cheng S et al. Identification of microbial markers across populations in early detection of colorectal cancer. *bioRxiv* 2020:2020.2008.2016.253344.
49. Rojas-Tapias DF, Brown EM, Temple ER, Onyekaba MA, Mohamed AMT, Duncan K, Schirmer M, Walker RL, Mayassi T, Pierce KA, et al. Inflammation-associated nitrate facilitates ectopic colonization of oral bacterium *Veillonella parvula* in the intestine. *Nat Microbiol*. 2022;7(10):1673–85.
50. Bertini I, Cacciatore S, Jensen BV, Schou JV, Johansen JS, Krühøffer M, Luchinat C, Nielsen DL, Turano P. Metabolomic NMR fingerprinting to identify and predict survival of patients with metastatic colorectal cancer. *Cancer Res*. 2012;72(1):356–64.
51. Rodríguez-Enríquez S, Robledo-Cadena DX, Gallardo-Pérez JC, Pacheco-Velázquez SC, Vázquez C, Saavedra E, Vargas-Navarro JL, Blanco-Carpintero BA, Marín-Hernández Á, Jasso-Chávez R, et al. Acetate promotes a Differential Energy metabolic response in human HCT 116 and COLO 205 Colon Cancer cells impacting Cancer Cell Growth and Invasiveness. *Front Oncol*. 2021;11:697408.
52. Ericksen RE, Lim SL, McDonnell E, Shuen WH, Vadeloo M, White PJ, Ding Z, Kwok R, Lee P, Radda GK, et al. Loss of BCAA catabolism during carcinogenesis enhances mTORC1 activity and promotes Tumor Development and Progression. *Cell Metab*. 2019;29(5):1151–e11651156.
53. Yang M, Soga T, Pollard PJ, Adam J. The emerging role of fumarate as an onco-metabolite. *Front Oncol* 2012, 2.
54. Cheng J, Yan J, Liu Y, Shi J, Wang H, Zhou H, Zhou Y, Zhang T, Zhao L, Meng X, et al. Cancer-cell-derived fumarate suppresses the anti-tumor capacity of CD8+ T cells in the tumor microenvironment. *Cell Metabol*. 2023;35(6):961–e978910.
55. Thomas AM, Manghi P, Asnicar F, Pasolli E, Armanini F, Zolfo M, Beghini F, Manara S, Karcher N, Pozzi C, et al. Metagenomic analysis of colorectal cancer datasets identifies cross-cohort microbial diagnostic signatures and a link with choline degradation. *Nat Med*. 2019;25(4):667–78.
56. Lee JS, Wang RX, Alexeev EE, Colgan SP. Intestinal inflammation as a dysbiosis of energy procurement: new insights into an old topic. *Gut Microbes*. 2021;13(1):1880241.
57. Yoshie T, Nishiumi S, Izumi Y, Sakai A, Inoue J, Azuma T, Yoshida M. Regulation of the metabolite profile by an APC gene mutation in colorectal cancer. *Cancer Sci*. 2012;103(6):1010–21.
58. Chhetri DR. Myo-Inositol and its derivatives: their emerging role in the treatment of Human diseases. *Front Pharmacol* 2019, 10.
59. Lin X, Hu T, Wu Z, Li L, Wang Y, Wen D, Liu X, Li W, Liang H, Jin X, et al. Isolation of potentially novel species expands the genomic and functional diversity of Lachnospiraceae. *iMeta*. 2024;3(2):e174.
60. Zhang X, Yu D, Wu D, Gao X, Shao F, Zhao M, Wang J, Ma J, Wang W, Qin X, et al. Tissue-resident Lachnospiraceae family bacteria protect against colorectal carcinogenesis by promoting tumor immune surveillance. *Cell Host Microbe*. 2023;31(3):418–e432418.
61. Vital M, Karch A, Pieper DH. Colonic Butyrate-Producing Communities in Humans: an Overview Using Omics Data. *mSystems* 2017, 2(6).

62. Giuliani G, Longo VD. Ketone bodies in cell physiology and cancer. *Am J Physiology-Cell Physiol.* 2024;326(3):C948–63.
63. Huang C, Tan H, Wang J, Huang L, Liu H, Shi Y, Zhong C, Weng S, Chen C, Zhao W, et al. β -hydroxybutyrate restrains colitis-associated tumorigenesis by inhibiting HIF-1 α -mediated angiogenesis. *Cancer Lett.* 2024;593:216940.
64. Salvi PS, Cowles RA. Butyrate and the intestinal epithelium: modulation of proliferation and inflammation in Homeostasis and Disease. *Cells* 2021, 10(7).
65. Kaiko GE, Ryu SH, Koues OI, Collins PL, Solnica-Krezel L, Pearce EJ, Pearce EL, Oltz EM, Stappenbeck TS. The Colonic Crypt protects stem cells from Microbiota-Derived metabolites. *Cell.* 2016;165(7):1708–20.
66. Yao N, Li W, Xu G, Duan N, Yu G, Qu J. Choline metabolism and its implications in cancer. *Front Oncol* 2023, 13.
67. Zhu R, Tang J, Xing C, Nan Q, Liang G, Luo J, Zhou J, Miao Y, Cao Y, Dai S et al. The distinguishing bacterial features from active and remission stages of Ulcerative Colitis revealed by Paired Fecal metagenomes. *Front Microbiol* 2022, 13.
68. Ye C, Liu X, Liu Z, Pan C, Zhang X, Zhao Z, Sun H. *Fusobacterium nucleatum* in tumors: from tumorigenesis to tumor metastasis and tumor resistance. *Cancer Biol Ther.* 2024;25(1):2306676.
69. Nissa MU, Pinto N, Ghosh B, Singh U, Goswami M, Srivastava S. Proteomic analysis of liver tissue reveals *Aeromonas hydrophila* infection mediated modulation of host metabolic pathways in *Labeo rohita*. *J Proteom.* 2023;279:104870.

Publisher's note

Springer Nature remains neutral with regard to jurisdictional claims in published maps and institutional affiliations.